First-principles investigation of the multilayer relaxation of stepped Cu surfaces

Juarez L. F. Da Silva, Kurt Schroeder, and Stefan Blügel
Institut für Festkörperforschung, Forschungszentrum Jülich, D-52425 Jülich, Germany
(Received 22 December 2003; published 25 June 2004)

We performed density-functional theory calculations, employing the all-electron full-potential linearized augmented plane-wave (FLAPW) method, for the multilayer relaxations of the vicinal, high-Miller-index Cu(210), Cu(211), and Cu(331) surfaces, as well as for the flat, low-Miller-index Cu(100), Cu(110), and Cu(111) surfaces. Generally, it is expected that the interlayer relaxation-sequence at stepped metal surfaces with n surface atom rows in the terraces exposed to the vacuum show $n-1$ contractions (indicated by $-$) followed by one expansion (indicated by $+$). However, recent studies based on low-energy electron diffraction (LEED) intensity analysis and all-electron FLAPW calculations suggested that the multilayer relaxation-sequence of the stepped Cu(331) surface, for which $n=3$, behaves anomalously, i.e., $-+\cdots$, instead of the expected $--+\cdots$. From the results presented in this work, we did not find any indication of such anomalous behavior for Cu(331) or for any of the investigated stepped Cu surfaces. For the flat surfaces we obtained the expected contraction of the topmost interlayer distance. In the particular case of the Cu(110) surface, a pronounced alternating oscillatory behavior extending over six interlayer distances was found, i.e., $-+-+-+$. For all studied Cu surfaces in the present work, we found a good quantitative agreement between our interlayer relaxations and those obtained by LEED intensity analysis.

DOI: 10.1103/PhysRevB.69.245411 PACS number(s): 68.47.De, 82.45.Jn, 71.15.Ap

I. INTRODUCTION

The creation of a surface significantly alters the electron density in the outermost surface layers. Thus, the surface atoms change their atomic positions due to the forces generated by the redistribution of the electron density, e.g., electrons smooth and spread themselves out in a way that weakens the electron-density corrugation mainly to lower their kinetic energy. Hence, the outermost surface atomic layers can shift perpendicular (inward or outward) and/or parallel to the surface, which gives rise to a change of the interlayer spacings. Furthermore, reconstructions of the surface might occur, i.e., the translational symmetry is changed.[1] The determination of the atomic structure of solid surfaces, i.e., the location of the atoms, and a microscopic understanding of the surface relaxations and reconstructions are among the basic questions in surface science due to the influence of the surface structure on many physical and chemical processes such as surface reactions, growth, and adsorption of adparticles (for a review see Ref. 2).

The understanding of these processes requires a microscopic understanding of surface defects, namely, adatoms, vacancies, steps, etc. In particular, steps are always present on real solid surfaces, e.g., even the Pt(111) surface has a density of atomic steps of 1% implying terrace widths of the order of 300 Å.[3] Surface atoms at the step edges change their atomic positions easier than other surface atoms due to their low coordination. Furthermore, steps provide preferential adsorption sites for adparticles. Thus, atomic steps affect a large number of surface properties such as morphology, reactivity, relaxations, etc. Therefore, there is a clear interest in understanding the structure of atomic steps at solid surfaces. To obtain that goal, the study of surfaces with periodic distribution of atomic steps, which are commonly called stepped surfaces, is the most simple and convenient approach.

For the past 30 years, the atomic structure of flat metal surfaces has been the subject of extensive studies by low-energy electron diffraction (LEED) intensity analysis and theoretical calculations,[4–22] however the study of the atomic structure of stepped metal surfaces is quite recent.[23–37] It has been found that *almost all* transition-metal surfaces show a contraction of the topmost interlayer spacing, and it increases with the openness of the surface. However, expansions of the topmost interlayer spacing have been reported for free-electronlike metal surfaces, e.g., Mg(0001),[20–22] Be(0001).[15]

The contraction of the topmost interlayer spacing on metal surfaces can be understood by the *physical* picture,[38] which relates the inward displacement to the Smoluchowski charge smoothing of the electron density,[39] while the expansion of the topmost interlayer spacing for surfaces such as Mg(0001) and Be(0001) is not as simple to explain as contraction of the topmost interlayer spacing. Feibelman[15] related the outward displacement of the topmost interlayer distance of Be(0001) and Mg(0001) to the demotion of electrons from p_σ- to s-states at the surface layer atoms, which have different magnitude for different surfaces. In both pictures, it is not straightforward to obtain information of the trends for multilayer relaxations, i.e., whether there is an interlayer contraction or expansion for the deep interlayer spacings.

For many metal systems the flat surfaces exhibit an alternating oscillatory behavior for the outermost interlayer spacing relaxations. For example, Adams *et al.*[7] reported an alternating behavior of the interlayer relaxation for Cu(110), i.e., $-+$, where the $-$ and $+$ signs indicate contractions and expansions, respectively, of the interlayer distance between two adjacent atomic layers parallel to the surface with respect to the unrelaxed surface. Their work was restricted only to the two topmost interlayer spacings. Thus, it is unclear whether this alternating behavior extends for several interlayer spacings into the bulk region.

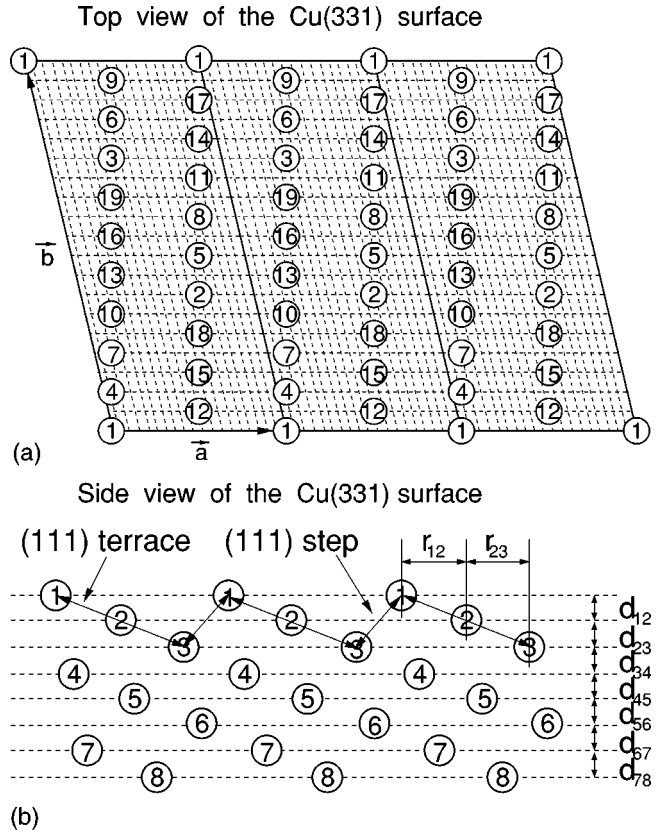

FIG. 1. Schematic diagram of the Cu(331) surface. The Cu atoms are indicated by open circles (decreasing for deeper layers) and the numbers indicate the layer number (increasing for deeper layers). (a) Top view. Directing the primitive vector $\vec{a}$ along the x axis, the primitive surface unit vectors are given by, $\vec{a}=(\sqrt{2}/2)a_0\vec{i}$, and $\vec{b}=-(\sqrt{2}/4)a_0\vec{i}+(\sqrt{38}/4)a_0\vec{j}$. The angle between the primitive vectors $\vec{a}$ and $\vec{b}$ is 102.921°. (b) Side view. The (111) terraces with three atom rows are indicated, as well as the monoatomic (111) steps. The interlayer spacing for the unrelaxed Cu(331) surface is given by $a_0/\sqrt{19}=0.833$ Å.

A different type of behavior has been found for the multilayer relaxation-sequence of stepped metal surfaces. Based on a large number of results for different stepped metal surfaces, obtained by quantitative LEED intensity analysis, first-principles calculations, and semiempirical calculations, it has been found that for a stepped metal surface exhibiting terraces with n atom rows exposed to the vacuum, the first $n-1$ interlayer spacings contract, while the nth interlayer distance expands.[32] For example, vicinal metal surfaces with a terrace width of 2, 3, and 4, atom rows exposed to the vacuum, the multilayer relaxation-sequences are $-+\cdots$, $--+\cdots$, and $---+\cdots$, respectively.

As shown in Fig. 1, the stepped Cu(331) surface has three atom rows in the (111) terraces exposed to the vacuum (indicated by numbers 1, 2, and 3), and a monoatomic (111) step. Therefore, a multilayer relaxation-sequence given by $--+\cdots$ is expected. The same behavior is also expected for stepped metal surfaces such as fcc(210), fcc(211), fcc(320), and fcc(511), which have also three atom rows in the terraces exposed to the vacuum. In the particular case of stepped Cu surfaces, this trend has been found true for Cu(210),[29,35,37] Cu(211),[25–27,30] and Cu(320).[33,36] However, experimental and theoretical results seem to indicate an irregular behavior for the Cu(331)[23,25,26,32,34] and Cu(511)[31] surfaces.

For Cu(331), independent semiempirical calculations based on the embedded-atom method (EAM)[25,26] and N-body effective potential (N-EP)[23] have obtained a multilayer relaxation-sequence given by $-+---$, instead of the expected $--+$. However, EAM calculations for geometrically similar stepped metal surfaces, e.g., Ag(331) and Pd(331), have obtained the expected trend $(--+)$.[26] Thus, based on the EAM and N-EP calculations, the Cu(331) surface has an irregular behavior compared with geometrically similar stepped transition-metal surfaces. Calculations based on the corrected effective-medium (CEM) theory performed by Sinnott *et al.*[24] obtained that the outermost two interlayer spacings contract, i.e., $--$. The sign of the relaxation of the third interlayer spacing (d_{34}) is unclear, since only the relaxation of the two outermost interlayer spacings were considered in their work.

Quantitative LEED intensity analysis performed by Tian *et al.*[32] obtained that the multilayer relaxation-sequence of Cu(331) is $-++-$. Thus, the LEED results seem to confirm the contraction and expansion of the two outermost interlayer spacings obtained by EAM and N-EP calculations,[23,25,26] but it is in disagreement with the CEM calculations.[24] However, Tian *et al.* obtained that the third interlayer distance expands, which is disagreement with the EAM and N-EP calculations. Based on their LEED results, Tian *et al.* suggested that there is an anomalous behavior for Cu(331) compared with geometrically similar stepped transition-metal surfaces, which follow the expected trend $(--+\cdots)$. The magnitude of the interlayer relaxations obtained by Tian *et al.* are $\Delta d_{12}=-13.8\pm4\%$, $\Delta d_{23}=+0.4\pm4\%$, and $\Delta d_{34}=+4\pm4\%$. The determination of the sign of the second interlayer spacing relaxation is a special issue as pointed out by Tian *et al.*, i.e., a large error (±4%) compared with the value itself (+0.4).

Density-functional theory (DFT) calculations, employing the all-electron full-potential linearized augmented plane-wave (FLAPW) method, reported by Geng and Freeman[34] also found that Cu(331) exhibits a multilayer relaxation-sequence given by $-++-\cdots$, which is in agreement with the LEED results obtained by Tian *et al.*[32] They obtained −22.0% for the interlayer relaxation of the topmost interlayer spacing, which is almost two times larger than the LEED result obtained by Tian *et al.*[32] Calculations for Cu(211) were also reported by Geng and Freeman.[34] They reported that the topmost interlayer spacing contracts by −28.4%, which is almost two times larger than the LEED result (−14.9%) obtained by Seyller *et al.*[30] However, first-principles calculations, employing the pseudopotential plane-wave (PPPW) approach, performed by Wei *et al.*[27] obtained a contraction of −14.4% for the topmost interlayer spacing of the Cu(210) surface, which is in close agreement with the contraction reported by Seyller *et al.*[30] Such large discrepancies between first-principle calculations based on DFT and LEED intensity analysis are rarely obtained nowadays.

Furthermore, we want to point out that the study of the atomic structure of stepped metal surfaces by LEED inten-

sity analyses and first-principles calculations is quite recently due to the complexity atomic structure of the stepped surfaces compared to the flat surfaces.[1] It has been reported that most of the computer programs used in the LEED intensity analysis have found problems with the quantitative analysis of the LEED intensities, when the interlayer distance is smaller than 1.0 Å,[28] which is the case of the Cu(210), Cu(211), and Cu(331) surfaces. Hence, the determination of the magnitude of the interlayer contractions and expansions for stepped surfaces is not as easy as for flat surfaces.

Therefore, first-principles calculations such as those performed with DFT, employing the all-electron FLAPW method or the PPPW approach, can be considered as decisive to provide the multilayer relaxations (magnitude and sequence) of high-Miller-index surfaces for interlayer distances smaller than 1.0 Å, since there is no restriction in such calculations with respect to the interlayer distance. However, first-principles calculations of multilayer relaxations, surface energy, work function, etc., for stepped metal surfaces are still computationally expensive nowadays due to the large size of the unit cell and large number of layers necessary to simulate a periodic sequence of terraces.

To verify if the suggested anomalous multilayer relaxation-sequence for the stepped Cu(331) surface, i.e., $-++$ instead of $--+$, is the physical behavior or an inaccuracy in the LEED intensity analyses and first-principles calculations, we performed careful first-principles DFT calculations, employing the all-electron FLAPW method. For comparison and to obtain a larger data base for providing an understanding of the multilayer relaxation phenomenon, we performed calculations also for the Cu(210) and Cu(211) surfaces. As an additional test of the quality of our FLAPW calculations, we studied the multilayer relaxation of the Cu(100), Cu(110), and Cu(111) surfaces.

This paper is organized as follows: In Sec. II, the theoretical approach and the computational details are described. In Sec. III, we present and discuss our results for the cohesive bulk Cu properties, interlayer contractions, and expansions of the low- and high-Miller-index Cu surfaces. Section IV summarizes the main conclusions, while in the Appendix we report the most important convergence tests performed in the present work.

II. METHOD

A. Theoretical approach

In this section we will describe the theoretical approach that we employed in our study, while the numerical parameters involved in the calculations will be reported in the next section. All calculations were performed using DFT[40,41] within the generalized gradient approximation proposed recently by Perdew *et al.*,[42] which is known as PBE functional, for the exchange-correlation energy functional. The Kohn-Sham equations are solved using the all-electron FLAPW method.[43] The core states are treated fully relativistically, while the semicore and valence states are treated by the scalar relativistic approximation, i.e., the spin-orbit coupling is neglected.

The LAPW wave functions in the interstitial region are represented using a plane-wave expansion truncated to include only plane-waves that have kinetic energies less than some particular cutoff energy, K^{wf}, and for the potential representation in the interstitial region plane-waves with wave vectors up to G^{pot} are considered. Inside the muffin-tin spheres with radius R_{mt}, the wave functions are expanded in radial functions times spherical harmonics up to $l_{\max}$, and for the representation of the potential inside the muffin-tin spheres, a maximum of $\tilde{l}_{\max}$ is used. For the evaluation of the nonspherical matrix elements of the Hamiltonian, we include terms up to $l_{\max}^{ns}$.

B. Computational details

All of the results that we are going to discuss in this paper were obtained with the all-electron FLAPW method as it is implemented in the FLEUR code.[44] This implementation includes total energy and atomic force calculations which allows a full structural optimization of bulk and surfaces. In the FLEUR code the solid surfaces are simulated using the approach proposed by Krakauer *et al.*,[45] i.e., a single slab (film) is sandwiched between two semi-infinite vacua. In the vacuum region the wave functions are described by a product of two-dimensional plane-wave and a *z*-dependent function. The vacuum wave functions are matched to the three-dimensional plane-waves of the interstitial region at a distance of $\pm D/2$ from the center of the slab.

To obtain the results that we show in this paper, we used the following set of numerical parameters: $K^{wf}=16.00$ Ry, $R_{\mathrm{mt}}^{\mathrm{Cu}}=1.16$ Å, $l_{\max}=9$, $G^{\mathrm{pot}}=273$ Ry, $\tilde{l}_{\max}=9$, and $l_{\max}^{ns}=6$, and $D=(N_l-1)d_0+4R_{mt}^{\mathrm{Cu}}$. d_0 is the interlayer spacing of the unrelaxed Cu surfaces and N_l is the number of atomic layers in the slab. The linearization energies E_l were set to be in the center of gravity of the occupied part of the band with the respective character (*s, p, d, f*,…). To improve the basis set, numerically calculated local-orbitals used to describe the semicore states,[46] were added to improve the description of the valence Cu 3*d*-states.

The bulk Cu was simulated using an tetragonal unit cell with two Cu atoms in the primitive cell. The primitive lattice vectors are $\vec{a}_1=(\sqrt{2}/2)a\vec{i}$, $\vec{a}_2=(\sqrt{2}/2)a\vec{j}$, and $\vec{a}_3=a\vec{k}$, where a is the lattice constant of the face-centered cubic lattice. For the integration over the bulk Brillouin zone (BZ) we used a $(14\times14\times10)$ Monkhorst-Pack grid,[47] i.e., 140 **k**-points in the irreducible part of the BZ. A broadening of the Fermi surface by the Fermi-Dirac distribution function with a broadening parameter, $k_{\mathrm{B}}T_{\mathrm{el}}=0.054$ eV was used. The total energy at zero temperature, i.e., $T_{\mathrm{el}}=0$ K, was obtained using the correction proposed by Gillan.[48] The theoretical equilibrium lattice constant, a_0, which was used in our surface calculations, was determined by minimization of the total energy with respect to the volume of the primitive unit cell. Calculations were performed for 17 regularly spaced volumes of the primitive unit cell.

The low- and high-Miller-index Cu surfaces were simulated using a (1×1) unit cell employing slabs with 7 to 20 Cu layers. To take advantage of the inversion symmetry

present in the Cu surfaces, which reduces computer time and memory requirements, both sides of the slab were relaxed. The integration over the surface BZ were performed using a two-dimensional Monkhorst-Pack **k**-mesh, namely, (14×14), (14×10), (14×14), (10×8), (14×6), (14×6), for the Cu(100), Cu(110), Cu(111), Cu(210), Cu(211), and Cu(331), surfaces, respectively. A broadening of the Fermi surface with $k_B T_{el}=0.054$ eV was used in all surface calculations. The effect of the broadening parameter on the surface properties was recently discussed by Da Silva[21] using the Pd(111) surface as an example. In the surface calculations, the atomic positions of the Cu atoms are determined by force minimization, in which the equilibrium configuration is assumed when the atomic force on each atom is smaller than 0.50 mRy/a.u. The dependence of the interlayer relaxations with respect to the cutoff energy, number of **k**-points in the irreducible part of the BZ, and to the parameter D is discussed in the Appendix for the particular case of the Cu(100) and Cu(110) surfaces.

III. RESULTS AND DISCUSSION

A. Cohesive bulk properties

The equilibrium lattice constant a_0 and the bulk modulus calculated at the equilibrium volume B_0 were obtained by fitting the total energy results to Murnaghan's equation of state.[49] To determine the cohesive energy E_{coh} for the bulk Cu, a spin-polarized total energy calculation for the free Cu atom was performed using a cubic box with a side length of 10.58 Å. Our results for the cohesive bulk Cu properties are, $a_0=3.63$ Å (55%), $B_0=1.38$ Mbar (0.73%), and $E_{coh}=-3.74$ eV (7.16%), while the experimental results are $a_0=3.61$ Å, $B_0=1.37$ Mbar, and $E_{coh}=-3.49$ eV.[50] The numbers in parentheses indicate the relative errors with respect to the experimental results. Our results are close to the experiments, as well as in agreement with other first-principles calculations employing the generalized gradient approximation, e.g., $a_0=3.62$ Å, $B_0=1.51$ Mbar,[51] $a_0=3.61$ Å,[19] $a_0=3.63$ Å, $B_0=1.42$ Mbar, and $E_{coh}=-3.51$ eV.[21,22]

B. Low-Miller-index Cu surfaces

The interlayer spacings were calculated with respect to the clean unrelaxed surface interlayer spacing, i.e., $\Delta d_{ij}=100(d_{ij}-d_0)/d_0$, where d_{ij} is the interlayer spacing between the layers i and j obtained by total energy minimization. d_0 is the interlayer spacing of the clean unrelaxed surface, e.g., $d_0=a_0/2=1.815$ Å, $\sqrt{2}\,a_0/4=1.283$ Å, and $\sqrt{3}\,a_0/3=2.096$ Å, for Cu(100), Cu(110), and Cu(111), respectively. For each low-Miller-index Cu surface, calculations were performed for two different numbers of layers in the slab, e.g., 11 and 7 for Cu(100) and Cu(111), and 13 and 7 for Cu(110). The magnitude of the interlayer relaxations are summarized in Table I, along with LEED results and previous theoretical calculations.

We found that the interlayer relaxations of the low-Miller-index Cu surfaces calculated using 13- and 11(-) layers thick slabs are almost the same as those calculated with 7-layers thick slabs. Thus, the results reported in Table I are converged with respect to the number of layers used to simulate the flat Cu surfaces. From now, only the results obtained with the largest number of layers for the flat Cu surfaces will be discussed.

For Cu(100), we found that the topmost interlayer spacing contracts, while the second interlayer spacing expands. These results are in qualitative agreement with LEED[8,10] and spin-polarized LEED (SP-LEED)[12] results. However, it can be seen in Table I that there is a deviation in the magnitude of the interlayer relaxations obtained by our FLAPW calculations and those obtained by LEED[8,10] and SP-LEED[12] intensity analysis. The contraction of the topmost interlayer spacing is larger by almost a factor of two compared with the LEED and SP-LEED results. The expansion of the second interlayer spacing is closer to the SP-LEED result, but smaller by almost a factor of two compared to the LEED results. Furthermore, we find that the two outermost interlayer relaxations are in agreement with previous DFT calculations, employing the PPPW approach, reported by Rodach *et al.*[16] However, there is a clear disagreement for Δd_{34}, i.e., we obtained an expansion while a contraction was reported.[16]

To investigate this discrepancy between DFT calculations and LEED intensity analysis results, the convergence of the interlayer relaxations with respect to the cutoff energy and to the number of **k**-points in the irreducible part of the surface BZ were checked (see Appendix). The reason for such deviation is not clear, but might be due to the presence of impurities on Cu(100) such as sulphur atoms. Very recent calculations (in progress) performed for the S/Cu(100) system for $1/4$ coverage indeed show that the topmost interlayer contraction is reduced, while the expansion of the second interlayer spacing increases, which is qualitatively in better agreement with the LEED results. However, new LEED intensity analysis for the flat Cu(100) might help to understand this discrepancy between DFT and LEED.

For Cu(110), we clearly found an alternating oscillatory behavior for the interlayer relaxation sequence, i.e., $-+-+-+$, which extends for six interlayer distances. This behavior was not observed for Cu(100) and Cu(111). The absolute values of the interlayer relaxations decrease with depth from the surface, i.e., $|\Delta d_{n,n+1}|>|\Delta d_{n+1,n+2}|$, which is intuitively expected, but not a rule. This behavior has not been observed by LEED studies yet, since only the topmost two interlayer relaxation parameters have been determined in earlier LEED intensity analysis studies.[4,5,7,9,10]

Table I shows a good agreement between our results and those obtained by LEED intensity analysis.[4,5,7,9,10] In fact, the agreement is much better than for Cu(100). Furthermore, our results are in excellent agreement with the results reported by Rodach *et al.*,[16] and Ross *et al.*,[18] while there are small discrepancies with the FLAPW calculations reported by Redinger *et al.*[14] They obtained a contraction of -6.2% for the topmost interlayer spacing, while we obtained -9.74%.

For Cu(111), we found that the first and second interlayer spacing contracts slightly, while the third interlayer spacing expands, i.e., $--+\cdots$, which contrasts to the oscillatory behavior found for Cu(110). The interlayer contraction of the topmost interlayer spacing is in close agreement with LEED

TABLE I. Multilayer relaxations, Δd_{ij}, of the Cu(100), Cu(110), and Cu(111) surfaces. N_l indicate the number of layers in the slab. $\Delta d_{ij}=100(d_{ij}-d_0)/d_0$, where d_{ij} is the interlayer spacing between the atomic layers i and j. d_0 is the interlayer spacing in the unrelaxed surface, i.e., $d_0=1.815$, 1.283, and 2.096 Å for Cu(100), Cu(110), and Cu(111), respectively. The + and − signs indicate expansion and contraction of the interlayer spacing, respectively.

Surface	N_l		Reference	Δd_{12} (%)	Δd_{23} (%)	Δd_{34} (%)	Δd_{45} (%)	Δd_{56} (%)	Δd_{67} (%)
Cu(100)	11	FLAPW	This work	−2.92	+0.70	+0.45	+0.12	−0.02	
	11	FLAPW	This work[a]	−2.52	+0.84	+0.68	+0.46	+0.51	
	7	FLAPW	This work	−2.89	+0.67	+0.38			
	7	FLAPW	This work [a]	−2.55	+1.00	+0.68			
	7	PPPW	[16]	−3.02	+0.08	−0.24			
		EAM	[13]	−1.41	−0.33				
		CEM	[24]	−6.2	+0.5				
		LEED	[10]	−1.10±0.40	+1.70±0.60				
		LEED	[8]	−1.00±0.40	+2.00±0.80				
		SP-LEED	[12]	−1.2	+0.9				
Cu(110)	13	FLAPW	This work	−9.74	+3.64	−1.17	+0.40	−0.09	+0.14
	7	FLAPW	This work	−9.64	+3.62	−0.77			
	11	FLAPW	[14]	−6.2	+2.1				
	7	FLAPW	[18]	−10.2	+3.8				
	7	PPPW	[16]	−9.27	+2.77	−1.08			
		EAM	[13]	−4.93	+0.23				
		EAM	[26]	−4.5	+0.2	−0.5			
		CEM	[24]	−15.0	+1.4				
		LEED	[7,9]	−8.5±0.6	+2.3±0.8				
		LEED	[4]	−10.0±2.5	0.0±2.5				
		LEED	[5]	−8±3					
		LEED	[10]	−7.90	+2.40				
Cu(111)	11	FLAPW	This work	−0.60	−0.18	+0.12	+0.40	+0.38	
	7	FLAPW	This work	−0.56	−0.45	+0.08			
	7	FLAPW	[21,22]	−1.19	−0.65	−0.24			
	9	FLAPW	[19]	−0.5	−0.3				
	7	PPPW	[16]	−1.27	−0.64	−0.26			
		EAM	[13]	−1.39	−0.05				
		CEM	[24]	−4.6	+0.5				
		LEED	[6]	−0.3±1					
		LEED	[11]	−0.7±0.5					
		V-LEED	[17]	$<+1.0$					

[a]Calculations using $K^{wf}=25.00$ Ry, instead of 16.00 Ry.

results,[6,11] however, our results do not support the expansion by almost 1% of the topmost interlayer spacing obtained by very-low-energy electron diffraction (V-LEED).[17] Furthermore, as was obtained for Cu(110) and Cu(100), our results are in agreement with the PPPW calculations reported by Rodach *et al.*[16] and FLAPW calculations reported by Bihlmayer *et al.*[19]

It can be seen in Table I that FLAPW calculations, employing the WIEN code, reported by Da Silva *et al.*[21,22] obtained a larger contraction for the topmost interlayer spacing and a contraction for the third interlayer spacing. To understand such differences, which is unexpected, since in both methods the same method is used, calculations were performed for Cu(111) using a large value for the parameter D. Using 7-layers thick slabs and $D=20.72$ Å, we obtained contractions of −0.80, −0.58, and −0.15% for the first, second, and third interlayer spacings, respectively, which are closer to the results reported by Da Silva *et al.*[21,22]

The quantitative agreement between our FLAPW calculations and those employing the embedded atom method (EAM)[13,26] and the corrected effective-medium (CEM) theory[24] is far from satisfactory. The topmost interlayer contraction for Cu(100), Cu(110), and Cu(111) calculated with the CEM theory are larger by almost a factor of two, while the results obtained with the EAM are smaller by almost a factor of two compared with our results.[13,24,26] Furthermore, for the cases, where the magnitude of the interlayer relaxation is of the order of 1.0%, there are deviations in the sign

of the relaxation, e.g., expansion is found instead of contraction. The potential used in the EAM is obtained by fitting experimental bulk data such as equilibrium volume, bulk modulus, elastic constants, cohesive energy, etc., i.e., the EAM results depend on fitting parameters, and hence, EAM studies are not as reliable and conclusive as first-principles calculations.

C. High-Miller-index Cu surfaces

The atomic structure of a stepped surface differs from the low-Miller-index surfaces in that it consists of an array of monoatomic steps separated by low-Miller-index terraces, as show in Fig. 1 for the particular case of the Cu(331) surface. Stepped surfaces such as Cu(331) are obtained by cutting a crystal along a plane at a small angle with respect to a principal low-Miller-index direction and the width of the terraces is the larger, the smaller the angle of the cut. Using the theoretical equilibrium lattice constant ($a_0=3.63$ Å), the interlayer distance, d_0, for Cu(210), Cu(211), and Cu(331) are $a_0/\sqrt{20}=0.812$ Å, $a_0/\sqrt{24}=0.741$ Å, and $a_0/\sqrt{19}=0.833$ Å, respectively, while for Cu(100), Cu(110), and Cu(111), $d_0=1.815$ Å, 1.283 Å, and 2.096 Å, respectively. Thus, the interlayer distance between two adjacent atomic layers parallel to the surface at high-Miller-index surfaces are considerably smaller than for the low-Miller-index surfaces.

In the stepped metal surfaces, opposite the flat surfaces where there are no relaxations parallel to the surface, there are relaxations parallel to the surface, which are called registry relaxations. The registry relaxations in the stepped surfaces studied in the present work occur perpendicular to the steps. The registry relaxations Δr_{ij} are defined similar to the interlayer relaxations perpendicular to the surface, i.e., $\Delta r_{ij}=100(r_{ij}-r_0)/r_0$, where r_{12}, r_{23}, and so on are indicated in Fig. 1. r_0 is the ideal registry interlayer distance of the unrelaxed surfaces, e.g., $r_0=(2\sqrt{5}/10)a_0=1.623$ Å, $(\sqrt{3}/3)a_0=2.096$ Å, and $(7\sqrt{38}/76)a_0=2.061$ Å for Cu(210), Cu(211), and Cu(331), respectively. The registry relaxations are smaller than the interlayer relaxations perpendicular to the surface, e.g., for Cu(210), the topmost registry relaxation obtained by LEED is $-1.83\pm3.0\%$, while the topmost interlayer contraction is $-11.12\pm2.0\%$.[35]

The LEED technique is not very sensitive to atomic displacements parallel to the surface. Thus, most of the reported LEED intensity analysis studies do not take in account the registry relaxations i.e., only the vertical interlayer relaxations are included in the fitting of the LEED intensities.[29,30,32,33] To verify the importance of the relaxations parallel to the surface in the interlayer relaxations perpendicular to the stepped surface, calculations were performed in two steps. In the first step, only relaxations perpendicular to the surface were included, while in the second step, relaxations perpendicular and parallel to the surface were included, i.e., the second step is a full geometric optimization. Furthermore, calculations were done using different numbers of layers for Cu(211) and Cu(331). Our results obtained for the interlayer and registry relaxations are summarized in Tables II and III, respectively, along with previous LEED and theoretical results.

We obtained that the interlayer relaxations of the Cu(211) and Cu(331) surfaces calculated with 13- and 12(-), layers thick slabs, respectively, are very close to the interlayer relaxations obtained with 19 and 20 layers thick slabs, respectively. The difference between the interlayer relaxations are close to 1.00%. Thus, it can be assumed that 13 layers in the slab are enough to obtain high accurate interlayer relaxations for open surfaces like the studied stepped Cu surfaces.

Furthermore, we found that the registry relaxations do no play any critical role in the sign of the interlayer relaxations, i.e., the multilayer relaxation-sequence does not change considering atomic displacements parallel to the surface, at least for the studied Cu surfaces. However, there are changes in the magnitude of the interlayer relaxations, mainly for the atoms close to the step edges, as can be seen in Table II. For example, we found that the contraction of the third interlayer spacing increases for *all* studied stepped metal surfaces upon registry relaxations.

We found that the multilayer relaxation-sequence for *all* studied stepped Cu surfaces with three exposed inequivalent atoms to the vacuum, e.g., Cu(210), Cu(211), and Cu(331), can be represented by $--+-\cdots$, i.e., the two topmost interlayer spacings contract, the third expands, and the fourth contracts. Thus, our results are in agreement with the trends observed for the multilayer relaxation-sequence of the stepped metal surfaces. Hence, we did not find any anomalous behavior in the multilayer relaxation-sequence of Cu(331). We hope that our results initiate LEED intensity analysis for Cu(331). From now, we will discuss the results obtained using the second step (full optimization) and the largest number of layers for each surface.

For Cu(210), the magnitude of the outermost interlayer relaxation is a bit larger than the available LEED intensity analysis results.[29,35,37] These LEED results reported by Ismail *et al.*[35] and Sun *et al.*[37] were obtained at a temperature of 130 K, while the results reported by Guo *et al.*[29] were obtained at room temperature. This might explain the larger difference between the experimental results. In contrast, the interlayer relaxation for the deeper layers is close to the LEED results. Furthermore, our results are in good agreement with recent theoretical calculations employing the ultrasoft PPPW method[37] and the projected augmented plane-wave (PAW) method[37] (see Table II).

The registry relaxations obtained by LEED intensity analysis are available only for the particular case of the Cu(210) surface. We found a registry relaxation-sequence given by $--+-$, which is in agreement with the LEED results reported in Refs. 35 and 37. Furthermore, there is quite good agreement with respect to the magnitude of the relaxations. Due to the small value of the relaxations differences between DFT and LEED is not surprising. However, we want to point out that the trend predicted by LEED intensity analysis is fully consistent with our results.

For Cu(211), the magnitude of the interlayer relaxations are in good agreement with the LEED results obtained at a temperature of 110 K by Seyller *et al.*[30] A good agreement is also obtained with the local-density approximation PPPW calculations performed by Wei *et al.*[27] However, our results are not in agreement with the all-electron FLAPW calculations performed by Geng and Freeman.[34] Their topmost in-

TABLE II. Multilayer relaxations Δd_{ij} of the Cu(210), Cu(211), and Cu(331) surfaces. N_l indicate the number of layers in the slab. $\Delta d_{ij}=100(d_{ij}-d_0)/d_0$, where d_{ij} is the interlayer spacing between the atomic layers i and j obtained by total energy minimization. d_0 is the interlayer spacing in the unrelaxed surface, i.e., $d_0=0.812$, 0.741, and 0.833 Å, for Cu(210), Cu(211), and Cu(331), respectively. The + and − signs indicate expansion and contraction of the interlayer spacing, respectively.

Surface	N_l	Reference	Δd_{12} (%)	Δd_{23} (%)	Δd_{34} (%)	Δd_{45} (%)	Δd_{56} (%)	Δd_{67} (%)	Δd_{78} (%)	Δd_{89} (%)
Cu(210)	15	This work[a]	−15.30	−4.57	+5.63	−1.18	+0.44	−1.07	+0.39	
	15	This work[b]	−15.93	−5.05	+6.45	−1.29	+0.04	−0.62	+0.29	
	21	[37]PPPW	−16.4	−4.5	+7.2	−0.6	−0.9	+1.4		
	21	[37]PAW	−17.1	−4.8	+7.0	−1.2	−0.9	+0.8		
		[24]CEM	−25.3	−4.7						
		[37]LEED	−11.1±1.9	−5.0±1.6	+3.7±1.7					
		[35]LEED	−11.12±2.0	−5.68±2.3	+3.83±2.5	+0.06±3.0	−0.66±3.5			
		[29]LEED	−5.7±5	−6.0±5	+6.8±4	−3.7±5	−0.5±4			
Cu(211)	13	This work[a]	−13.84	−7.03	+7.74	−1.92	−2.13	+1.19		
	13	This work[b]	−13.24	−9.80	+9.39	−1.93	−1.91	+1.23		
	13	This work[c]	−13.05	−8.32	+6.50	−1.82	−2.78	+0.55		
	19	This work[a]	−13.20	−7.27	+7.78	−2.24	−1.76	+1.56	+0.11	−0.90
	19	This work[b]	−13.17	−9.43	+9.19	−2.04	−1.17	+1.17	+0.26	−0.74
	15	[34]FLAPW	−28.4±1	−3.0±1	+15.3±1	−6.6±1	+0.7±1	+3.0±1	0.0±1	
	17	[27]PPPW	−14.4	−10.7	+10.9	−3.8	−2.3	+1.7	−1.0	
	72	[25]EAM	−10.28	−5.41	+7.26	−5.65	−1.2	+3.99	−2.6	
		[26]EAM	−10.3	−5.1	+7.3	−5.6	−1.1			
		[30]LEED	−14.9±4.1	−10.8±4.1	+8.1±4.1					
Cu(331)	12	This work[a]	−12.10	−3.46	+5.84	−2.75	+0.67			
	12	This work[b]	−13.09	−5.04	+7.54	−2.65	+0.67			
	20	This work[a]	−12.25	−3.35	+5.33	−2.99	+0.65	+0.31	−0.13	+0.31
	20	This work[b]	−14.23	−3.95	+6.59	−2.80	+0.17	+0.21	+0.29	−0.07
	20	This work[c]	−13.18	−3.17	+4.64	−3.35	+0.57	−0.32	−0.36	
	13	[34]FLAPW	−22.0±1	+1.6±1	+6.9±1	−2.4±1	−0.6±1	−0.4±1		
	72	[25]EAM	−10.42	+1.72	−1.66	−0.27	−0.3	+0.54	−0.37	
		[26]EAM	−10.5	+2.0	−1.5	−0.4	−0.2			
		[24]CEM	−18.9	−5.7						
		[23]*N*-EP	−8.8	+2.7	−1.8	−0.1				
		[32]LEED	−13.8±4	+0.4±4	+4.0±4	−4.0±4				

[a]Only relaxations perpendicular to the surface were included in the force optimization.
[b]Relaxations parallel and perpendicular to the surface were included in the force optimization.
[c]Using the same parameters used by Geng and Freeman (Ref. 34), e.g., $K^{wf}=13$ Ry (only perpendicular relaxations).

terlayer relaxation is two times larger than our result.

For Cu(331), we found good agreement between our results and those obtained by quantitative LEED intensity analysis reported by Tian *et al.*[32] for Δd_{12} and Δd_{34}. However, the same agreement is not obtained for Δd_{23}. Our calculations predict a contraction, while LEED intensity analysis found an expansion. It can be seen in Table II that the error in the LEED intensity analysis is larger than the value itself and our result is inside of the given range. As for the Cu(211) surface, our results are not in good agreement with the FLAPW results obtained by Geng and Freeman.[34] For example, their result for the topmost interlayer relaxation is $-22.0\pm1\%$, which is almost two times larger than our result. Geng and Freeman obtained an expansion for the second interlayer distance, $\Delta d_{23}=+1.6\pm1\%$, while we obtained a contraction.

The source of the difference between our results and those reported by Geng and Freeman[34] is unclear, since the same method was used in both calculations. To understand the differences we performed test calculations for the Cu(211) and Cu(331) surfaces using the same set of parameters as used by Geng and Freeman, e.g., $K^{wf}=13$ Ry, etc. We found that the interlayer relaxations change slightly (see Table II), but the trend did not change. Therefore, our tests calculations could not identify the source of the differences between our results and those by Geng and Freeman.[34] Since we carefully checked the convergence of the interlayer relaxations of the Cu surfaces with respect to the cutoff energy and number of

TABLE III. Registry relaxations, Δr_{ij}, for the Cu(210), Cu(211), and Cu(331) surfaces. The + and − signs indicate expansion and contraction of the registry spacings, respectively.

	Cu(210)	Cu(211)		Cu(331)	
%	$N_l=15$	$N_l=13$	$N_l=19$	$N_l=12$	$N_l=20$
Δr_{12}	−0.98	−1.86	−1.77	−1.04	−0.81
Δr_{23}	−0.67	−0.93	−0.95	−1.70	−1.78
Δr_{34}	+2.08	−0.63	−0.56	+1.44	+1.52
Δr_{45}	−0.47	+1.72	+1.80	+0.90	+0.55
Δr_{56}	−0.76	−0.35	−0.25	−0.39	−0.39
Δr_{67}	+0.11	+0.52	+0.34		+0.24
Δr_{78}	+0.11		+0.01		−0.11
Δr_{89}			−0.18		+0.01

k-points in the irreducible part of the BZ, as well as with respect to the number of layers in the slab, we believe that our results are correct.

To complete the discussion for Cu(331), we find good agreement between our results and those obtained by EAM[25,26] for the topmost interlayer spacing. However, the same agreement is not obtained for Δd_{23} and Δd_{34}. The EAM calculations yield an expansion and a contraction by a few percent, while our calculations predict a contraction and an expansion for Δd_{23} and Δd_{34}, respectively. The results obtained with CEM[24] are in good agreement with our results for the first and second interlayer spacing relaxations. Such differences are to be expected since these methods are based on nonfree-parameter ionic potentials fitted to bulk properties.

The contraction of the topmost interlayer spacing of low- and high-Miller-index Cu surfaces can be explained by the Smoluchowski charge smoothing of the electron-density.[38,39] On a real solid surface, electrons smooth and spread themselves out mainly to lower their total kinetic energy. This weakens the electron-density corrugation and means that the electron density flows from the region above the atoms (on-top site region) to the region between them (hollow site region), which in turn creates a layer of positive ion cores. Thus, electrostatic forces cause the topmost surface plane to move inwards, i.e., resulting in a contraction of the topmost interlayer spacing.

Thus, for solid surfaces with a large electron-density corrugation such as the fcc(110) surface, the contraction of the topmost interlayer spacing is larger than for the more closely packed fcc(111) surfaces, which is indeed obtained by LEED intensity analysis and first-principles calculations. It is important to note that this explanation does not take in account the difference in the nature of the chemical bonding in the different metal surfaces.

For stepped surfaces several atom rows on the terraces (which belong to different planes) are in direct contact with the vacuum region. These atoms are affected by the Smoluchowski charge smoothing of the electron-density, and hence, a contraction is obtained for several interlayer spacings, whose number depends on the number of atom rows in the terraces, which is in fact obtained in our calculations. However, this picture cannot be used to determine the multilayer relaxations for deeper atomic layers, i.e., cannot predict the full multirelaxation sequence.

IV. SUMMARY

In the present work we performed DFT calculations, employing the all-electron FLAPW method, for the low- and high-Miller-index Cu surfaces, namely, the Cu(100), Cu(110), Cu(111), Cu(210), Cu(211), and Cu(331) surfaces.

For the low-Miller-index surfaces, we obtained good agreement between our results and the LEED intensity analysis for the (110) and (111) Cu surfaces, however, the same level of agreement was not obtained for the Cu(100) surface. We attribute this to the possible presence of impurities on the surface, e.g., sulfur atoms. Very recent calculations (in progress) performed for the S/Cu(100) system for $1/4$ coverage indeed show that the topmost interlayer contraction is reduced, while the expansion of the second interlayer spacing increases, which qualitatively is in better agreement with the LEED results. Furthermore, we obtained a clearly alternating oscillatory behavior for the interlayer contractions and expansions sequence for Cu(110), i.e., $-+-+-+\cdots$, while for the Cu(100) and Cu(111) surfaces different multilayer relaxation-sequences were obtained, e.g., $-++\cdots$ and $--+\cdots$, respectively.

We found that the stepped surfaces Cu(210), Cu(211), and Cu(331), with three exposed surface atoms on the terrace, have the same multilayer relaxation-sequence, i.e., $--+-\cdots$. The contraction of the two topmost interlayer spacings are in accordance with the sequence expected from the Smoluchowsky corrugation smoothing[38,39] for stepped surfaces with three atom rows in the terrace. Therefore, based on our all-electron FLAPW calculations, there is no anomalous behavior for the multilayer relaxation of the Cu(331) surface as was suggested in the literature.[32,34]

Furthermore, we obtained that the registry relaxations do not play any role for the sign of the interlayer relaxations perpendicular to the surface, however, they are important for the correct magnitude of the interlayer relaxations involving atoms close to the step edges. In general, we found good agreement between our all-electron FLAPW calculations and the interlayer relaxations obtained with LEED intensity analysis, however, discrepancies between DFT and LEED still exist for particular cases, e.g., Cu(100) and Cu(331). We expect that such discrepancies can originate new LEED intensity analysis studies of Cu surfaces.

ACKNOWLEDGMENT

The authors would like to thank G. Bihlmayer for his help with the FLEUR code.

APPENDIX

Here we will discuss the dependence of the interlayer relaxations, Δd_{ij}, of the Cu(100) and Cu(110) surfaces with respect to computational parameters such as the cutoff energy K^{wf} and number of **k**-points in the irreducible part of the BZ, $N^{\mathbf{k}}_{\mathrm{IBZ}}$. For the particular case of the Cu(110) surface,

TABLE IV. Interlayer relaxations, Δd_{ij} of the Cu(100) and Cu(100) surfaces as a function of the cutoff energy K^{wf} and to the number of **k**-points in the irreducible part of the BZ $N^{\mathbf{k}}_{\mathrm{IBZ}}$. The correspondent two-dimensional **k**-point meshes are indicated in parentheses. Δd_{ij} is calculated with respect to the interlayer distance of the unrelaxed ideal surface. The + and − signs indicate expansion and contraction of the interlayer spacing, respectively.

	Cu(100)				Cu(110)		
K^{wf} (Ry)	Δd_{12} (%)	Δd_{23} (%)	Δd_{34} (%)	K^{wf} (Ry)	Δd_{12} (%)	Δd_{23} (%)	Δd_{34} (%)
10.56	−5.83	−2.02	−2.56	10.56	−11.93	+1.80	−3.02
12.25	−4.14	−0.15	−0.47	12.25	−10.46	+2.89	−1.61
14.06	−3.34	+0.55	+0.34	14.06	−9.92	+3.37	−1.04
16.00	−2.89	+0.67	+0.38	16.00	−9.64	+3.62	−0.77
18.06	−2.85	+0.90	+0.60	18.06	−9.44	+3.79	−0.58
20.25	−2.66	+0.98	+0.54	20.25	−9.28	+3.78	−0.52
22.56	−2.58	+0.98	+0.67	22.56	−9.19	+3.75	−0.59
25.00	−2.55	+1.00	+0.68	25.00	−9.22	+3.75	−0.56
	Cu(100)				Cu(110)		
$N^{\mathbf{k}}_{\mathrm{IBZ}}$	Δd_{12} (%)	Δd_{23} (%)	Δd_{34} (%)	$N^{\mathbf{k}}_{\mathrm{IBZ}}$	Δd_{12} (%)	Δd_{23} (%)	Δd_{34} (%)
10 (8×8)	−2.80	+0.62	−0.03	6 (6×4)	−8.95	+3.78	−0.54
15 (10×10)	−2.84	+1.03	+1.00	12 (8×6)	−9.62	+3.00	−0.76
21 (12×12)	−3.00	+0.48	+0.41	15 (10×6)	−9.65	+4.19	−0.64
28 (14×14)	−2.89	+0.67	+0.38	24 (12×8)	−9.35	+3.66	−0.41
36 (16×16)	−2.96	+0.65	+0.26	35 (14×10)	−9.64	+3.62	−0.77
45 (18×18)	−2.79	+0.56	+0.41	48 (16×12)	−9.49	+3.77	−0.63
55 (20×20)	−2.92	+0.60	+0.25	54 (18×12)	−9.63	+3.70	−0.79

calculations were performed also as a function of the parameter D, which separates the slab (film) to the semi-infinite vacuum region at both sides of the slab. It can be seen in Table I that 7 layers in the slab are enough to obtain converged interlayer relaxations for the flat surfaces. Thus, our test calculations were performed employing 7-layers thick slabs for the Cu(100) and Cu(110) surfaces. The results are summarized in Tables IV and V.

For both surfaces, calculations were performed for eight different values for the cutoff energy in the range from 10.56 to 25.00 Ry. These calculations were performed using (14×14) and (14×10) two-dimensional **k**-point meshes for Cu(100) and Cu(110), respectively. We obtained that the cutoff energy plays an important role in the magnitude and sign of the interlayer relaxations. For example, using $K^{wf}=10.56$ Ry, we found that the topmost interlayer spacing contracts by −6.09 and −12.18% for the Cu(100) and Cu(110) surfaces, respectively, however, using a cutoff energy of 25.00 Ry, we obtained that $\Delta d_{12}=-2.55$ and −9.22% for Cu(100) and Cu(110), respectively. For the deep interlayer spacings of Cu(100), which have small interlayer relaxations, the correct sign of the interlayer relaxation is obtained only for cutoff energies higher than 14.06 Ry.

Furthermore, for both surfaces, calculations were performed for seven different sets of **k**-points using 16.00 Ry as the cutoff energy. We found that the number of **k**-points used to perform the integration over the BZ does not play an important role on the interlayer relaxations.

The Cu(110) surface was simulated with 7 layers in the slab, hence, the minimum value for the parameter D is 10.02 Å, which depends on the interlayer distance (1.283 Å) and sphere Cu radius (1.16 Å) by the following equation, $D=6d_0+2R^{\mathrm{Cu}}_{mt}$. Calculations were performed using seven different values for the parameter D, which were obtained using the following equation, $D=6d_0+nR^{\mathrm{Cu}}_{mt}$, where $n=2$, 3, 4, 5, 6, 7, and 8, respectively. These calculations were performed using $K^{wf}=16.00$ Ry and $N^{\mathbf{k}}_{\mathrm{IBZ}}=35$. We obtained that the parameter D does not play a critical role in the interlayer relaxations. The changes in the interlayer relaxations are almost negligible for values of D larger than 12.36 Å.

From the test calculations reported in the present Appendix we can conclude that a cutoff energy of 16.00 Ry is sufficient to obtain well converged interlayer relaxations for

TABLE V. Interlayer relaxations Δd_{ij} of the Cu(110) surface as a function of the parameter D (see text). $D=6d_0+nR^{\mathrm{Cu}}_{mt}$ and Δd_{ij} is calculated with respect to the interlayer distance of the unrelaxed ideal surface d_0. The + and − signs indicate expansion and contraction of the interlayer spacing, respectively.

n	D (Å)	Δd_{12} (%)	Δd_{23} (%)	Δd_{34} (%)
2	10.02	−9.29	+3.65	−0.64
3	11.18	−9.49	+3.55	−0.85
4	12.36	−9.64	+3.62	−0.77
5	13.52	−9.58	+3.49	−0.90
6	14.68	−9.59	+3.50	−0.87
7	15.84	−9.62	+3.47	−0.94
8	17.00	−9.59	+3.48	−0.93

Cu(110), but not for the Cu(100) surface, which requires a larger cutoff energy. A large number of **k**-points were used in our final calculations discussed in the present paper, e.g., 28 and 35 **k**-points in the irreducible part of the BZ, due to the fact that we also calculated the surface energy for the mentioned surfaces which is going to be discussed in a further publication. Similar high quality **k**-point sets were used in all other surface calculations. For the particular case of the parameter D, our calculations for the Cu(110) surface indicate that $D=12.36$ Å, are sufficient to obtain converged results. For the parameter D, which depends on the number of layers in the slab, we used the following relation, $D=(N_l-1)d_0=4R_{mt}^{\mathrm{Cu}}$ to determine D for all surface calculations reported in the present paper.

[1] M.-C. Desjonquères and D. Spanjaard, *Concepts in Surface Science* (Springer, New York, 1995).
[2] For a retrospective of surface science, see Surf. Sci. **500**, 1 (2002).
[3] W. Widdra, P. Trischberger, W. Frieß, and D. Menzel, Phys. Rev. B **57**, 4111 (1998).
[4] H. L. Davis, J. R. Noonan, and L. H. Jenkins, Surf. Sci. **83**, 559 (1979).
[5] J. R. Noonan and H. L. Davis, Surf. Sci. **99**, L424 (1980).
[6] S. P. Tear, K. Röll, and M. Prutton, J. Phys. C **14**, 3297 (1981).
[7] D. L. Adams, H. B. Nielsen, J. N. Andersen, I. Stensgaard, R. Feidenhans, and L. E. Sorensen, Phys. Rev. Lett. **49**, 669 (1982).
[8] J. R. Noonan and H. L. Davis, Bull. Am. Phys. Soc. **27**, 237 (1982).
[9] D. L. Adams, H. B. Nielsen, and J. N. Andersen, Surf. Sci. **128**, 294 (1983).
[10] H. L. Davis and J. R. Noonan, Surf. Sci. **126**, 245 (1983).
[11] S. Å. Lindgren, L. Walldén, J. Rundgren, and P. Westrin, Phys. Rev. B **29**, 576 (1984).
[12] D. M. Lind, F. B. Dunning, G. K. Walters, and H. L. Davis, Phys. Rev. B **35**, 9037 (1987).
[13] S. M. Foiles, M. I. Baskes, and M. S. Daw, Phys. Rev. B **33**, 7983 (1986).
[14] J. Redinger, P. Weinberger, H. Erschbaumer, R. Podloucky, C. L. Fu, and A. J. Freeman, Phys. Rev. B **44**, 8288 (1991).
[15] P. J. Feibelman, Phys. Rev. B **46**, 2532 (1992).
[16] Th. Rodach, K.-P. Bohnen, and K. M. Ho, Surf. Sci. **286**, 66 (1993).
[17] I. Bartoš, P. Jaroš, A. Barbieri, M. A. van Hove, W. F. Chung, Q. Cal, and M. S. Altman, Surf. Sci. Lett. **2**, 477 (1995).
[18] Ch. Ross, B. Schirmer, M. Wuttig, Y. Gauthier, G. Bihlmayer, and S. Blügel, Phys. Rev. B **57**, 2607 (1998).
[19] G. Bihlmayer, Ph. Kurz, and S. Blügel, Phys. Rev. B **62**, 4726 (2000).
[20] Ismail, Ph. Hofmann, A. P. Baddorf, and E. W. Plummer, Phys. Rev. B **66**, 245414 (2002), and references therein.
[21] J. L. F. Da Silva, *The Nature and Behavior of Rare-Gas Atoms on Metal Surfaces*. Ph.D. thesis (http://edocs.tu-berlin.de/diss/2002/dasilva_juarez.htm or http://www.fhi-berlin.mpg.de/th/pub02.html), Technical University Berlin, Berlin, Germany, 2002.
[22] J. L. F. Da Silva, C. Stampfl, and M. Scheffler (unpublished).
[23] B. Loisel, D. Gorse, V. Pontikis, and J. Lapujoulade, Surf. Sci. **221**, 365 (1989).
[24] S. B. Sinnott, M. S. Stave, T. J. Raeker, and A. E. DePristo, Phys. Rev. B **44**, 8927 (1991).
[25] S. Durukanoğlu, A. Kara, and T. S. Rahman, Phys. Rev. B **55**, 13894 (1997).
[26] I. Y. Sklyadneva, G. G. Rusina, and E. V. Chulkov, Surf. Sci. **416**, 17 (1998).
[27] C. Y. Wei, Steven P. Lewis, E. J. Mele, and A. M. Rappe, Phys. Rev. B **57**, 10062 (1998).
[28] F. Jona, Surf. Sci. Lett. **6**, 621 (1999).
[29] Y. P. Guo, K. C. Tan, A. T. S. Wee, and C. H. A. Huan, Surf. Sci. Lett. **6**, 819 (1999).
[30] Th. Seyller, R. D. Dihl, and F. Jona, J. Vac. Sci. Technol. A **17**, 1635 (1999).
[31] D. A. Walko and I. K. Robinson, Phys. Rev. B **59**, 15446 (1999).
[32] Y. Tian, K.-W. Lin, and F. Jona, Phys. Rev. B **62**, 12844 (2000).
[33] Y. Tian, J. Quinn, K.-W. Lin, and F. Jona, Phys. Rev. B **61**, 4904 (2000).
[34] W. T. Geng and A. J. Freeman, Phys. Rev. B **64**, 115401 (2001).
[35] Ismail, S. Chandravakar, and D. M. Zehner, Surf. Sci. **504**, L201 (2002).
[36] S. Durukanoğlu and T. S. Rahman, Phys. Rev. B **67**, 205406 (2003).
[37] Y. Y. Sun, H. Xu, J. C. Zheng, J. Y. Zhou, Y. P. Feng, A. C. H. Huan, and A. T. S. Wee, Phys. Rev. B **68**, 115420 (2003).
[38] M. W. Finnis and V. Heine, J. Phys. F: Met. Phys. **4**, L37 (1974).
[39] R. Smoluchowski, Phys. Rev. **60**, 661 (1941).
[40] P. Hohenberg and W. Kohn, Phys. Rev. **136**, B864 (1964).
[41] W. Kohn and L. J. Sham, Phys. Rev. **140**, A1133 (1965).
[42] J. P. Perdew, S. Burke, and M. Ernzerhof, Phys. Rev. Lett. **77**, 3865 (1996).
[43] D. J. Singh, *Plane Waves, Pseudopotentials and LAPW Method* (Kluwer Academic, Boston, 1994).
[44] http://www.flapw.de
[45] H. Krakauer, M. Posternak, and A. J. Freeman, Phys. Rev. B **19**, 1706 (1979).
[46] D. J. Singh, Phys. Rev. B **43**, 6388 (1991).
[47] H. J. Monkhorst and J. D. Pack, Phys. Rev. B **13**, 5188 (1976).
[48] M. G. Gillan, J. Phys.: Condens. Matter **1**, 689 (1989).
[49] F. D. Murnaghan, Proc. Natl. Acad. Sci. U.S.A. **50**, 697 (1944).
[50] C. Kittel, in *Introduction to Solid State Physics*, 7th ed. (Wiley, New York, 1996).
[51] A. Khein, D. J. Singh, and C. J. Umrigar, Phys. Rev. B **51**, 4105 (1995).